ARTICLES

Noise-resistant and synchronized oscillation of the segmentation clock

Kazuki Horikawa[1]*, Kana Ishimatsu[1]*, Eiichi Yoshimoto[2]*, Shigeru Kondo[2] & Hiroyuki Takeda[1]

Periodic somite segmentation in vertebrate embryos is controlled by the 'segmentation clock', which consists of numerous cellular oscillators. Although the properties of a single oscillator, driven by a *hairy* negative-feedback loop, have been investigated, the system-level properties of the segmentation clock remain largely unknown. To explore these characteristics, we have examined the response of a normally oscillating clock in zebrafish to experimental stimuli using *in vivo* mosaic experiments and mathematical simulation. We demonstrate that the segmentation clock behaves as a coupled oscillator, by showing that Notch-dependent intercellular communication, the activity of which is regulated by the internal *hairy* oscillator, couples neighbouring cells to facilitate synchronized oscillation. Furthermore, the oscillation phase of individual oscillators fluctuates due to developmental noise such as stochastic gene expression and active cell proliferation. The intercellular coupling was found to have a crucial role in minimizing the effects of this noise to maintain coherent oscillation.

Synchronized oscillation is a universal feature of many biological systems, such as the fluorescent 'blinking' of fireflies or the rhythmic cellular activities of the neuronal and cardiac systems[1,2]. A transcriptional oscillator that is responsible for vertebrate somitogenesis, known as the segmentation clock, also displays synchronized oscillation (Fig. 1 and Supplementary Notes S1)[3–5]. The segmentation clock is an ensemble of numerous cellular oscillators, located in the unsegmented pre-somitic mesoderm (PSM). The travelling wave generated from the synchronized oscillation in the posterior PSM sweeps anteriorly and arrests around the future segmentation point during the formation of each somite (every 30 min in zebrafish; see also Supplementary Notes S1)[3,6]. It is believed that the frequency of this clock oscillation controls the size of the resulting segments (Supplementary Notes S2)[7–9], although no direct evidence for this has been shown. Previous genetic analyses suggested that the segmentation clock can be considered as a coupled oscillator, wherein numerous cellular oscillators, driven by negative-feedback regulation of *hairy*-related transcriptional repressors[10–14], are coupled by oscillator-linked Notch-mediated intercellular communication (Box 1 and Supplementary Notes S1)[15,16]. However, because of the complex network of genes that function both intra- and intercellularly, we are still far from having a complete understanding of the mechanisms controlling the collective behaviour of the segmentation clock (that is, the synchronized oscillations, or the travelling and arresting waves, including their transition in the oscillation modes).

In the present study we have focused on the mechanisms of synchronized oscillation, which is the earliest and most basic mode of oscillation generated in the posterior PSM (Fig. 1). In particular, we asked how the intercellular communication coordinates individual cellular oscillators and maintains a global oscillation pattern. By using zebrafish embryos, we experimentally and mathematically analysed the system-level response of the normal oscillator to experimental stimuli.

Acceleration of clock oscillation induced by *her*-MO cells

To understand better the function of Notch signalling in the segmentation clock, we examined how the normal oscillators respond to activated Notch signalling. In this assay, we unilaterally transplanted genetically modified cells at the blastula stage into the marginal mesoderm that was fated to become the somite, then analysed the effects of explants upon both the segment positions and the oscillation pattern of *her1* (zebrafish *hairy-related gene1*) at the segmentation stage (Fig. 2a). We first examined the effect of non-oscillating cells with high levels of Notch ligands on host segmentation. These donor cells were obtained from embryos in which the translation of *her1* and *her7* had been inhibited by morpholino anti-sense oligonucleotides (*her*-MO cells). *her*-MO cells are expected to continuously activate Notch signalling in surrounding cells, because the expression of *deltaC* is upregulated due to the absence of Her1/7-dependent repression (Supplementary Notes S1)[10,14]. The results of this experiment were striking: in most of the transplanted embryos (91 out of 96) the segment positions were anteriorly shifted on the transplanted side (Fig. 2b). In addition, the segment size was locally reduced around the explants. This segment-shift activity of *her*-MO cells was also found to depend upon the function of DeltaC, as its depletion in donor cells abolishes the segment-shift activity of *her*-MO cells (Fig. 2c). This is also the case for DeltaD[17], another ligand for Notch broadly expressed in the posterior PSM (data not shown).

The expression of molecular markers in the *her*-MO-cell mosaic embryos revealed that oscillation of the segmentation clock is specifically affected on the transplanted side (Fig. 2d, f), whereas the level of FGF signalling in the PSM, which also regulates segment positions[18,19], is unchanged (Supplementary Notes S2). *her1* expression is maintained in a segmental pattern on both sides of these transplanted embryos, but becomes out of phase such that the oscillation of the transplanted side advances relative to that of the control side (Fig. 2d–g and Supplementary Notes S2). This result indicates that the oscillation phase is accelerated by *her*-MO cells. Consistently, when donor cells are localized either laterally or medially in the PSM, the shape of the *her1* stripes becomes flattened

[1]Department of Biological Sciences, Graduate School of Science, University of Tokyo, Hongo 7-3-1, Tokyo 113-0033, Japan. [2]Division of Biological Science, Graduate School of Science, Nagoya University, Furo-cho, Nagoya 464-8602, Japan.
*These authors contributed equally to this work.

(Fig. 2d) or medially tilted (Fig. 2f), supporting the idea that *her*-MO cells locally accelerate *her1* oscillation in adjacent cells. Notably, expression of *her1* is already affected in the posterior-most synchronized oscillation zone (bracket in Fig. 2f) as well as in the travelling wave zone (intermediate and anterior PSM), indicating that the interaction between normally oscillating host and *her*-MO donor cells occurs in the posterior PSM. Indeed, high-resolution *in situ* hybridization (ISH) clearly demonstrates that the timing of *her1* transcription is locally advanced in cells that surround the transplanted *her*-MO cells in the posterior PSM (Fig. 2h, i). Furthermore, the intercellular communication that accelerates *her1* oscillation is certainly active in the synchronized oscillation zone, because the same results were obtained when *her*-MO cells were directly transplanted into the posterior PSM of normal host: segment positions and *her1* expression were locally shifted around the transplanted cells (Supplementary Notes S2). Thus, Notch-dependent intercellular communication accelerates the phase of neighbouring oscillators *in vivo*.

The 'phase acceleration' that we observed in the *in vivo* experiment is a general response of a coupled oscillator system. Indeed, local acceleration of an oscillating system by actively signalling cells is reproduced in our numerical simulation (for details, see Box 1, Supplementary Notes S3 and Supplementary Movie S1).

We conclude that the segmentation clock behaves as a coupled oscillator, in which cellular oscillators are interconnected through oscillator-linked Notch signalling.

Fluctuations in individual oscillators

In the segmentation clock, the period and phase of individual oscillators might fluctuate for the following reasons. Rhythm-generating reactions such as transcription, translation and translocation of key factors are in themselves stochastic processes at the molecular level[20–22]. Furthermore, the dynamics of these processes can be affected by mitosis, during which the transcription and translation of most genes are arrested[23]. Changes in cell shape during cell division may also alter the efficiency of contact-dependent intercellular communication that could potentially affect the oscillation period. Indeed, we have observed active cell proliferation in the synchronized oscillation zone (Fig. 3a). Time-lapse analysis of embryos expressing a histone 2B–green fluorescent protein (GFP) fusion gene revealed that during one cycle of oscillation, 10–15% of cells experience the mitotic phase (M phase), which lasts at least 15 min (Fig. 3b, Supplementary Table S1 and Supplementary Movie S2). Moreover, given the remarkably short period of *her1* oscillation (30 min), the presence of numerous dividing cells with the 15-min M phase might not be negligible for coherent oscillation.

To test whether the cyclic expression of segmentation genes actually fluctuates *in vivo*, we determined the phase of oscillating cells in the synchronized oscillation zone using high-resolution ISH. As described above, cells in this zone repeat the ON/OFF cycle in almost complete synchrony. However, a certain proportion of these cells were out of phase (Fig. 3c); for example, some cells prematurely initiate *her1* transcription in a transcriptionally silent population (arrowhead in Fig. 3d) and others still retain *her1* messenger RNA in the cytoplasm as their surrounding cells become negative for its presence (arrow in Fig. 3e). The presence of slightly advanced and slightly delayed cells indicates that *her1* oscillation fluctuates in individual cells, and this may be caused by stochastic gene expression. Stochastic transcription in each allele within a cell can be detected by the differential distribution of exonic and intronic probes for *her1*. As is shown in Fig. 3f, one allele is being transcribed (positive for both intronic and exonic probes; arrowhead) while transcription in

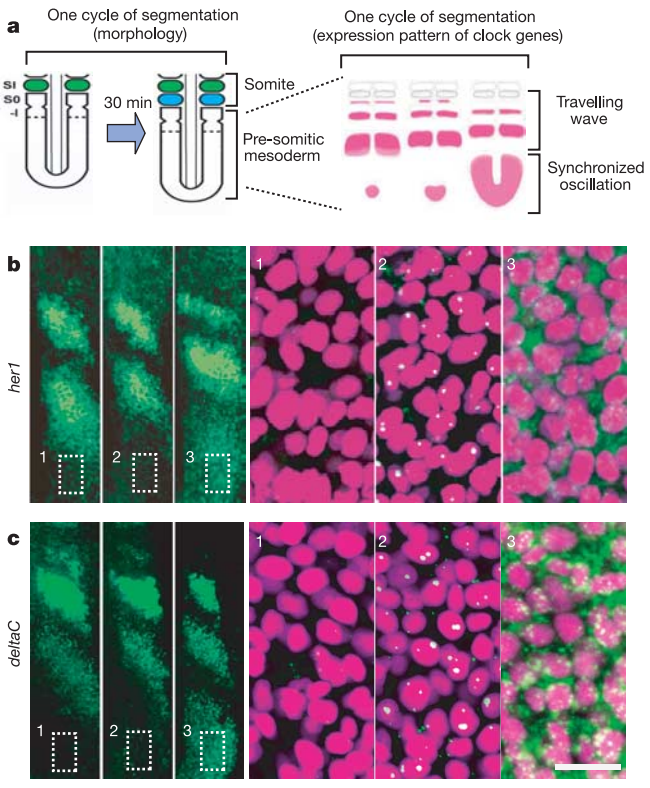

Figure 1 | Synchronized oscillation of *her1* and *deltaC* in the posterior PSM. **a**, Schematic representation of the clock oscillation during one segmentation cycle. **b**, **c**, Subcellular localization of *her1* (**b**) and *deltaC* (**c**) mRNA (green) visualized by high-resolution ISH. PSM cells display one of the following patterns of mRNA localization: no signal, nuclear dots or cytoplasmic localization, representing states with no transcripts, with active transcription, or with active translation, respectively. Numbered insets are enlarged in the panels to the right; see also Supplementary Notes S1. Magenta indicates nuclei. Scale bar, 20 μm.

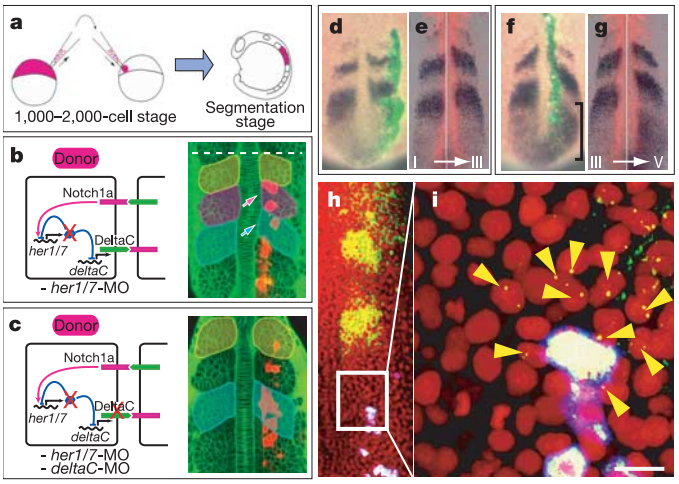

Figure 2 | Effects of actively signalling cells upon synchronized oscillation. **a**, Cell-transplantation assay at the blastula stage. **b**, Affected segment positions in a *her*-MO-cell mosaic embryo. The dashed line indicates the last normally formed segment border. **c**, Rhodamine-labelled donor cells doubly injected with *deltaC*-MO and *her*-MO do not affect segment positions. Tissue morphology is outlined by Bodipy-ceramide staining. **d**, **f**, *her1* expression (purple) in mosaic embryos that received *her*-MO cells (green). **e**, **g**, Composite images of normal *her1* expression patterns (purple) arranged so as to represent **d** and **f**. Note that the pattern on the right side is advanced compared with that on the left (see also Supplementary Notes S2). **h**, **i**, The timing of *her1* transcription is locally advanced in the area near to the explants in the posterior PSM. Nuclei, *her1* mRNA and explants are stained red, green and blue, respectively. Arrowheads indicate nuclear *her1*-positive cells. Scale bar, 20 μm.

another allele is just terminated (positive only for exonic probes; arrow). This contrasts with the nucleus, which shows active transcription in both alleles (asterisk in Fig. 3f). Furthermore, some asynchronous cells can be found in pairs (arrows in Fig. 3g). This raises the possibility that they are sibling cells generated by a recent cell division. In support of this idea, we did not detect *her1* transcripts in either condensed or segregating chromatin even though the surrounding cells were synchronously initiating *her1* transcription (Fig. 3h, i). These data indicate that internal noise caused by both stochastic gene expression and cell division affects the oscillation period of unit oscillators, as is often seen for other biological oscillators[24,25].

Coupling-assisted coherent oscillation against noise

The effects of noise must be minimized to maintain coherent oscillation, and it is thought that intercellular coupling has a role in this process, as is the case for other 'noisy' biological systems[1,2,26]. To understand the importance of Notch signalling for coherent oscillation, we cultured embryos in the presence of the γ-secretase inhibitor DAPT to reduce Notch activity. Wild-type embryos at the 6-somite stage were transiently treated with DAPT or DMSO for the next four cycles of oscillation, and subjected to high-resolution ISH. This treatment greatly affected *her1* synchrony in the posterior PSM, although the overall expression patterns were less affected under these experimental conditions (Fig. 4a, b). In DAPT-treated embryos, the cellular localization of *her1* mRNA became variable from cell to cell (Supplementary Fig. S10) and the proportion of nuclear *her1*-positive cells was approximately 20–30% at every phase of oscillation, whereas that of the control embryos shifted from 10% to 90%, depending on the phase. Similar results were obtained by our numerical simulation in which 25 PSM cells oscillate in the presence of noise with or without intercellular coupling (Box 1 and Supplementary Notes S3). Thus, *in vivo* and *in silico* experiments demonstrate the presence of the Notch-dependent phase synchronization mechanism in the segmentation clock.

The phase synchronization was directly tested by a cell-transplantation experiment. To juxtapose two independently oscillating populations, we isolated a group of cells from the posterior PSM of a wild-type donor and directly transplanted them into another wild-type host at the same axial level (Fig. 4c). After several rounds of oscillation, the oscillation phase of the explants, some of which must have been originally out of phase, became synchronized

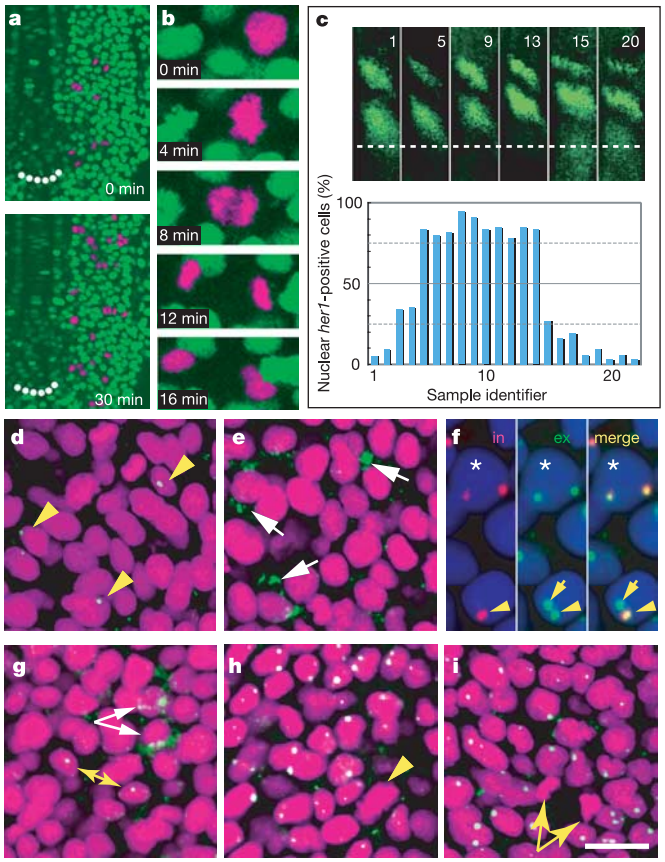

Figure 3 | Fluctuated oscillation of *her1*. **a**, **b**, Mitosis in the posterior PSM. Nuclei (histone 2B–GFP) that experienced mitosis during one cycle of oscillation are labelled magenta (pseudo-coloured). White dots indicate the posterior end of the axial mesoderm. **c**, The percentage of nuclear *her1*-positive cells in 22 specimens of posterior PSM (posterior to the dashed line). Specimen numbers are indicated. **d**, **e**, A few of the nuclear *her1*-positive (arrowheads in **d**) or cytoplasmic *her1*-positive cells (arrows in **e**) are detectable even in the OFF-state PSM. **f**, Nuclear localization of premature and fully matured *her1* transcripts, detected by intronic (in, red) and exonic (ex, green) probes, respectively. **g**, Pairs of asynchronous cells. **h**, **i**, Absence of *her1* transcripts in either condensed or segregating chromatin. All *her1* mRNA is detected by exonic probes except for **f**. Anterior is to the top. Scale bar, 20 μm.

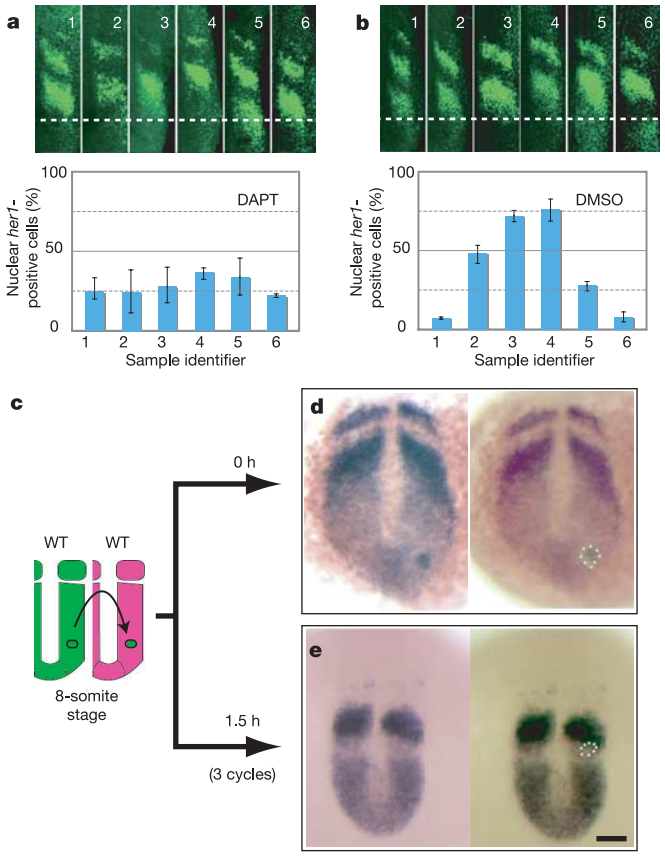

Figure 4 | Coupling-assisted phase synchronization. **a**, **b**, Synchrony in 10-somite-stage embryos transiently treated with DAPT (**a**) or DMSO (**b**) for 2 h, starting at the 6-somite stage. Representative expression patterns of *her1* and its synchrony (posterior to the dashed line) are shown. Error bars indicate the range of scores taken from three different *z*-positions in one PSM sample. **c**–**e**, Synchronization of out-of-phase explants. **c**, Wild-type cells of the posterior PSM were directly transplanted into normal embryos at the same axial level. **d**, **e**, *her1* expression (purple in the left and right panels) in these embryos just after transplantation (**d**) or 1.5 h later (**e**) is shown. At the time of transplantation, 9 out of 22 explants exhibit an oscillation phase that is different from that of the host, whereas 24 out of 26 are in phase after three rounds of oscillation. The position of biotin-labelled donor cells is detected as green staining (encircled with white dots in the right panels). Scale bar, 50 μm.

with that of the host (Fig. 4d, e; see also Supplementary Notes S3 and Supplementary Movie S3 for simulation), indicating that phase synchronization actually works in the segmentation oscillator.

We conclude that Notch-dependent intercellular coupling is crucial for the maintenance of synchronized oscillation, by reducing the effects of internal noise in the PSM.

Discussion

By using a simple model with a minimum number of components, we have experimentally shown that the segmentation clock behaves as a typical coupled oscillator that displays strong robustness to developmental noise. However, an *in vivo* oscillation mechanism must be much more complicated than we have assumed here[27]. We observed that simple overexpression of DeltaC and DeltaD proteins (either or both) is not sufficient for PSM explants to exert the segment-shift activity (data not shown), suggesting that an as-yet-unidentified factor(s) functions downstream of Her1/7 in parallel with Delta proteins. Fringe (a modulator of Notch signalling[6,28,29]) or the Wnt pathway[30], both of which are essential in other vertebrate species, might be such factors. However, the minimum model that we used was very informative in understanding the system-level properties of the clock. Recently, several groups demonstrated that simplification of the dynamics of a few representative elements, although neglecting molecular details, can provide valuable information about the behaviour of biological systems[31–33]. The present study could be one such case.

It is noteworthy that vertebrate embryos use a robust system for developmental pattern formation, which has a primary function to establish a reproducible pattern in a proliferating population of cells. In this context, one may recall the classical concept of developmental biology, canalization, in which living organisms produce a standard phenotype with surprisingly few variations under different environmental and genetic conditions[34]. This has raised the important issue of how such a developmental programme can be so resistant to various perturbations[35,36]. This phenomenon has been partially explained by the presence of redundant elements and by self-balancing feedback regulation, which mainly functions at the level of local circuit[37–39]. At the same time, it has been theoretically suggested that higher-order mechanisms, driven by system-level dynamics, could also ensure the stability of the genetic programme, as exemplified by the wide ranging tolerance of variation of the initial conditions during the segmentation programme in *Drosophila*[40,41]. In our current study, we demonstrate that such higher-order mechanisms—phase synchronization and mutual entrainment—ensure the coherent oscillation of the segmentation clock, even in the presence of proliferating cells. This work therefore presents a novel molecular explanation for the mechanisms underlying developmental canalization.

Box 1 | Modelling of Notch-coupled oscillators

To assess the results obtained in the *in vivo* experiments, we numerically examined the phase dynamics of the segmentation clock *in silico*. The oscillation dynamics shown in the following simulation (see below) is common among coupled oscillator systems and does not depend on the driving mechanism of oscillation. Here, we adopt the 'delay model' (ref. 16), simply because the model has been most supported by molecular and genetic experiments of the segmentation clock[44] (see also Supplementary Notes S1 and S3). In this model, cell-autonomous oscillation is explained by the dynamics of mRNA and protein concentration of the transcriptional repressors *her1* and *her7*, incorporating the 'delay time' for their maturation.

We simulated oscillation in a one-dimensional array of virtual PSM cells coupled by Notch–Delta communication, as shown in Box 1 Fig. 1. Delta protein expressed in one cell is evenly distributed on both sides. Thus, the Notch signal in one cell is activated by Delta protein expressed in neighbouring cells on both sides. (For details of the simulation, see Supplementary Notes S3.)

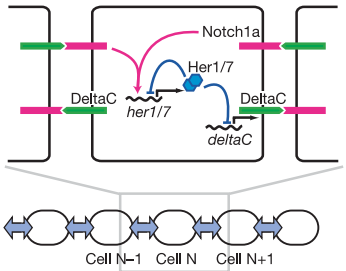

Box 1 Figure 1 | Molecular network of the segmentation clock.

To simulate the phase-shift effect induced by *her*-MO cells, we put a cell that constantly expresses high levels of Delta protein at the right end of the one-dimensional array of ten cells (Box 1 Fig. 2). The active signal from the transplanted cell influences the adjacent cell to accelerate the oscillating phase (13.4% of the oscillation phase after 500 min; see also Supplementary Fig. S7). This effect is transmitted in succession, and results in the phase shift of relatively distant cells, although the effect is still locally limited. (For details, see Supplementary Notes S3 and Supplementary Movie S1.)

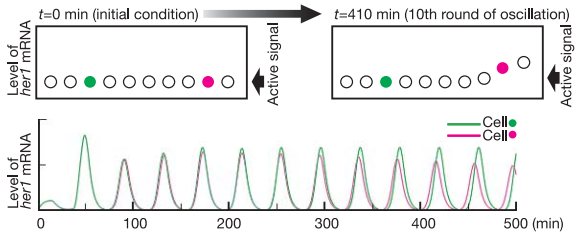

Box 1 Figure 2 | Phase acceleration by activated Notch signalling.

Next, we tested the importance of intercellular coupling in the presence of noise. Based on the experimental observations (Fig. 3), the effect of noise is introduced as follows. Effect 1 is distributed frequency in each oscillator. Here, delay time for all components in each cell is distributed with the standard deviation value of 0.15 and is fixed throughout the simulation. Effect 2 is phase shift associated with mitosis. Here, dividing cells are randomly selected such that 7% of cells in a total population experience mitosis during one cycle of oscillation. During the division (supposed to last for 15 min), the delay time is doubled and the synthesis rate of mRNAs and proteins is set to half the value. At time 0, all the cells in the array oscillate synchronously. Without the coupling (up), the phase of oscillation soon becomes random. However, with coupling (down), the cell array can maintain the coherent oscillation (Box 1 Fig. 3). (For details, see Supplementary Notes S3.)

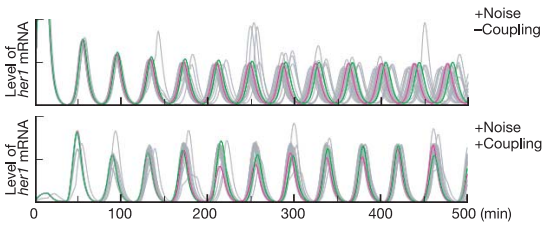

Box 1 Figure 3 | Oscillation pattern in a 25-cell array.

METHODS

High-resolution ISH and image analysis. To preserve the cellular localization of mRNAs, embryos were fixed with 4% PFA for 2 h at room temperature. During the course of the study, we found that ice-cold fixative never produced nuclear signals. DIG- or FITC-labelled cRNA probes were detected with TSA-Alexa488 (Molecular Probes: T-20932) or TSA-Alexa647 (Molecular Probes: T-20936), according to the manufacturer's instructions and ref. 42. Detailed procedure is also described in ref. 43. To determine the numbers of nuclear *her1*-positive cells, whole PSMs of flat-mounted embryos were optically scanned at 1-μm intervals (Olympus: FV500). PSM cells located at the levels between the 5th and 15th adaxial cells from the posterior end were subjected to this analysis. Three distinct *z*-positions in each PSM were sterically analysed using Volocity (Improvision). The values from each assessment were analysed graphically using Microsoft Excel.

Time-lapse imaging of mitosis. To visualize mitosis in the posterior PSM, embryos were injected with histone 2B–EGFP mRNA ($100\,ng\,\mu l^{-1}$) at the one-cell stage. Embryos mounted in an LMP-agarose gel were time-lapse imaged with a confocal microscope (Olympus: FV500) for 30 min. Each PSM was scanned with six optical slices (10-μm thickness) at 1-min intervals and *z*-stack images at each time point were processed for movies using Photoshop and ImageReady (Adobe).

Detailed description of other methods including cell transplantation and DAPT treatment are provided in Supplementary Methods.

Received 26 October 2005; accepted 5 May 2006.

1. Winfree, A. T. Biological rhythms and the behavior of populations of coupled oscillators. *J. Theor. Biol.* **16,** 15–42 (1967).
2. Winfree, A. T. *The Geometry of Biological Time* (Springer, New York, 2000).
3. Palmeirim, I., Henrique, D., Ish-Horowicz, D. & Pourquié, O. Avian hairy gene expression identifies a molecular clock linked to vertebrate segmentation and somitogenesis. *Cell* **91,** 639–648 (1997).
4. Pourquié, O. The segmentation clock: converting embryonic time into spatial pattern. *Science* **301,** 328–330 (2003).
5. Saga, Y. & Takeda, H. The making of the somite: molecular events in vertebrate segmentation. *Nature Rev. Genet.* **2,** 835–845 (2001).
6. Dale, J. K. *et al.* Periodic notch inhibition by lunatic fringe underlies the chick segmentation clock. *Nature* **421,** 275–278 (2003).
7. Cooke, J. Control of somite number during morphogenesis of a vertebrate, *Xenopus laevis*. *Nature* **254,** 196–199 (1975).
8. Cooke, J. & Zeeman, E. C. A clock and wavefront model for control of the number of repeated structures during animal morphogenesis. *J. Theor. Biol.* **58,** 455–476 (1976).
9. Cooke, J. A gene that resuscitates a theory—somitogenesis and a molecular oscillator. *Trends Genet.* **14,** 85–88 (1998).
10. Holley, S. A., Julich, D., Rauch, G. J., Geisler, R. & Nusslein-Volhard, C. her1 and the notch pathway function within the oscillator mechanism that regulates zebrafish somitogenesis. *Development* **129,** 1175–1183 (2002).
11. Hirata, H. *et al.* Oscillatory expression of the bHLH factor Hes1 regulated by a negative feedback loop. *Science* **298,** 840–843 (2002).
12. Bessho, Y., Hirata, H., Masamizu, Y. & Kageyama, R. Periodic repression by the bHLH factor Hes7 is an essential mechanism for the somite segmentation clock. *Genes Dev.* **17,** 1451–1456 (2003).
13. Henry, C. A. *et al.* Two linked hairy/Enhancer of split-related zebrafish genes, her1 and her7, function together to refine alternating somite boundaries. *Development* **129,** 3693–3704 (2002).
14. Oates, A. C. & Ho, R. K. Hairy/E(spl)-related (Her) genes are central components of the segmentation oscillator and display redundancy with the Delta/Notch signaling pathway in the formation of anterior segmental boundaries in the zebrafish. *Development* **129,** 2929–2946 (2002).
15. Jiang, Y. J. *et al.* Notch signalling and the synchronization of the somite segmentation clock. *Nature* **408,** 475–479 (2000).
16. Lewis, J. Autoinhibition with transcriptional delay: a simple mechanism for the zebrafish somitogenesis oscillator. *Curr. Biol.* **13,** 1398–1408 (2003).
17. Holley, S. A., Geisler, R. & Nusslein-Volhard, C. Control of her1 expression during zebrafish somitogenesis by a delta-dependent oscillator and an independent wave-front activity. *Genes Dev.* **14,** 1678–1690 (2000).
18. Sawada, A. *et al.* Fgf/MAPK signalling is a crucial positional cue in somite boundary formation. *Development* **128,** 4873–4880 (2001).
19. Dubrulle, J., McGrew, M. J. & Pourquié, O. FGF signaling controls somite boundary position and regulates segmentation clock control of spatiotemporal Hox gene activation. *Cell* **106,** 219–232 (2001).
20. McAdams, H. H. & Arkin, A. Stochastic mechanisms in gene expression. *Proc. Natl Acad. Sci. USA* **94,** 814–819 (1997).
21. Shav-Tal, Y. *et al.* Dynamics of single mRNPs in nuclei of living cells. *Science* **304,** 1797–1800 (2004).
22. Blake, W. J., Kærn, M., Cantor, C. R. & Collins, J. J. Noise in eukaryotic gene expression. *Nature* **422,** 633–637 (2003).
23. Prescott, D. M. & Bender, M. A. Synthesis of RNA and protein during mitosis in mammalian tissue culture cells. *Exp. Cell Res.* **26,** 260–268 (1962).
24. Nagoshi, E. *et al.* Circadian gene expression in individual fibroblasts: cell-autonomous and self-sustained oscillators pass time to daughter cells. *Cell* **119,** 693–705 (2004).
25. Welsh, D. K., Yoo, S. H., Liu, A. C., Takahashi, J. S. & Kay, S. A. Bioluminescence imaging of individual fibroblasts reveals persistent, independently phased circadian rhythms of clock gene expression. *Curr. Biol.* **14,** 2289–2295 (2004).
26. Ueda, H. R., Hirose, K. & Iino, M. Intercellular coupling mechanism for synchronized and noise-resistant circadian oscillators. *J. Theor. Biol.* **216,** 501–512 (2002).
27. Rida, P. C., Le Minh, N. & Jiang, Y. J. A Notch feeling of somite segmentation and beyond. *Dev. Biol.* **265,** 2–22 (2004).
28. Evrard, Y. A., Lun, Y., Aulehla, A., Gan, L. & Johnson, R. L. *lunatic fringe* is an essential mediator of somite segmentation and patterning. *Nature* **394,** 377–381 (1998).
29. Zhang, N. & Gridley, T. Defects in somite formation in *lunatic fringe*-deficient mice. *Nature* **394,** 374–377 (1998).
30. Aulehla, A. *et al.* Wnt3a plays a major role in the segmentation clock controlling somitogenesis. *Dev. Cell* **4,** 395–406 (2003).
31. Ma'ayan, A. *et al.* Formation of regulatory patterns during signal propagation in a mammalian cellular network. *Science* **309,** 1078–1083 (2005).
32. Brandman, O., Ferrell, J. E. Jr, Li, R. & Meyer, T. Interlinked fast and slow positive feedback loops drive reliable cell decisions. *Science* **310,** 496–498 (2005).
33. Bornholdt, S. Systems biology. Less is more in modeling large genetic networks. *Science* **310,** 449–451 (2005).
34. Waddington, C. Canalization of development and the inheritance of acquired characters. *Nature* **150,** 563–565 (1942).
35. Houchmandzadeh, B., Wieschaus, E. & Leibler, S. Establishment of developmental precision and proportions in the early *Drosophila* embryo. *Nature* **415,** 798–802 (2002).
36. Lucchetta, E. M., Lee, J. H., Fu, L. A., Patel, N. H. & Ismagilov, R. F. Dynamics of *Drosophila* embryonic patterning network perturbed in space and time using microfluidics. *Nature* **434,** 1134–1138 (2005).
37. Freeman, M. Feedback control of intercellular signalling in development. *Nature* **408,** 313–319 (2000).
38. Eldar, A. *et al.* Robustness of the BMP morphogen gradient in *Drosophila* embryonic patterning. *Nature* **419,** 304–308 (2002).
39. Hall, B. K. & Olson, W. M. *Keywords and Concepts in Evolutionary Developmental Biology* (Harvard Univ. Press, Cambridge, Massachusetts, 2003).
40. von Dassow, G., Meir, E., Munro, E. M. & Odell, G. M. The segment polarity network is a robust developmental module. *Nature* **406,** 188–192 (2000).
41. Ingolia, N. T. Topology and robustness in the *Drosophila* segment polarity network. *PLoS Biol.* **2,** e123 (2004).
42. Kosman, D. *et al.* Multiplex detection of RNA expression in *Drosophila* embryos. *Science* **305,** 846 (2004).
43. Julich, D. *et al.* beamter/deltaC and the role of Notch ligands in the zebrafish somite segmentation, hindbrain neurogenesis and hypochord differentiation. *Dev. Biol.* **286,** 391–404 (2005).
44. Hirata, H. *et al.* Instability of Hes7 protein is crucial for the somite segmentation clock. *Nature Genet.* **36,** 750–754 (2004).

Supplementary Information is linked to the online version of the paper at www.nature.com/nature.

Acknowledgements We thank T. Fujimori for providing human histone 2B–EGFP cDNA; D. Tautz for the technical advice regarding the synthesis of intronic probes for *her1*; T. Tomita and T. Iwatsubo for their gift of DAPT; and Y. J. Jiang for Notch1a mutant (des^{th35b}). We also thank H. Ueda, T. Uemura, M. Takeichi, A. Takamatsu and J. Lewis for their advice and for critical reading of the manuscript. This work was supported by a postdoctoral fellowship and in part by Grants-in-Aid for Scientific Research Priority Area Genome Science and Organized Research Combination System, both of which are from the Ministry of Education, Culture, Sports, Science and Technology of Japan.

Author Information Reprints and permissions information is available at npg.nature.com/reprintsandpermissions. The authors declare no competing financial interests. Correspondence and requests for materials should be addressed to K.H. (kazu@biol.s.u-tokyo.ac.jp) or H.T. (htakeda@biol.s.u-tokyo.ac.jp).